

Article

Sand Dune Height Increases Water Use Efficiency at the Expense of Growth and Leaf Area in Mongolian Pine Growing in Hulunbeier Steppe, Inner Mongolia, China

Chan-Beom Kim ^{1,2} , Yong Suk Kim ¹ , Hyung Tae Choi ¹, Jeonghwan Kim ¹, Seongjun Kim ³, Sangsub Cha ¹ , Guang-Lei Gao ⁴ , Yan-Feng Bao ⁵, Yowhan Son ², Jino Kwon ^{1,†} and Ki-Hyung Park ^{1,*} 

¹ Division of Forest Conservation & Restoration, National Institute of Forest Science, Seoul 02455, Korea

² Department of Environmental Science and Ecological Engineering, Graduate school, Korea University, Seoul 02841, Korea

³ Institute of Life Science and Natural Resources, Korea University, Seoul 02841, Korea

⁴ College of Soil & Water Conservation, Beijing Forestry University, Beijing 100083, China

⁵ Institute of Desertification Studies, Chinese Academy of Forestry, Beijing 100091, China

* Correspondence: bear1127@korea.kr; Tel.: +82-0296-1264-7

† Forest Biomaterials Research Center, National Institute of Forest Science, 52817 Jinju, Korea; alp96jk@korea.kr

Received: 28 May 2019; Accepted: 2 July 2019; Published: 3 July 2019



Abstract: The Mongolian pine (*Pinus sylvestris* var. *mongolica*) is one of the most common tree species in semiarid and arid areas of China, especially in the sand dunes of the Hulunbeier steppe. This study addresses the morphological and physiological characteristics of the Mongolian pine according to sand dune height. Five sites were chosen with various sand dune heights (P1–P5). Nine years after planting, tree growth, leaf area, leaf mass per leaf unit area (LMA), diameter at breast height (DBH), tree height, diameter at root collar (DRC), longest shoot length, carbon isotope composition, and intrinsic water use efficiency (iWUE) were measured to explore the responses of Mongolian pine trees to drought. DBH, tree height, DRC, leaf area, leaf length, and longest shoot length significantly decreased with greater sand dune height ($p < 0.05$). However, the carbon isotope actually increased with dune height ($p < 0.05$). Conversely, the iWUE of current-year pine needles was significantly higher at measurement points P3 ($132.29 \mu\text{mol CO}_2 \text{ mol}^{-1} \text{ H}_2\text{O}$), P4 ($132.96 \mu\text{mol CO}_2 \text{ mol}^{-1} \text{ H}_2\text{O}$), and P5 ($125.34 \mu\text{mol CO}_2 \text{ mol}^{-1} \text{ H}_2\text{O}$) than at the lower points P1 ($95.18 \pm 9.87 \mu\text{mol CO}_2 \text{ mol}^{-1} \text{ H}_2\text{O}$) and P2 ($103.10 \pm 11.12 \mu\text{mol CO}_2 \text{ mol}^{-1} \text{ H}_2\text{O}$). Greater sand dune height increases the distance to groundwater, which in this study led to an increase in iWUE in the Mongolian pines, thus these trees appear to adapt to increased sand dune height by increasing their iWUE and decreasing their leaf area. However, prolonged periods characterized by such adaptations can lead to tree death. We expect these findings to be useful when selecting plantation sites for Mongolian pines in semiarid and arid climates.

Keywords: carbon isotope composition; grassland; sand dune; soil moisture; water use efficiency

1. Introduction

Desertification is a growing environmental problem that currently affects at least one-third of the world's landmass [1]. Desertification exacerbates socioeconomic and environmental issues, such as lack of food security, poverty, and the reduction or loss of biodiversity [1]. Currently, the arid zone created by desertification contains more than 1 billion people who are living in poor conditions [2].

Over 2.622 million km² of land in China, accounting for 27.3% of the total area of the country, has been affected by desertification [3]. From 1981 to 2010, desertification in North China significantly increased, driven by both climate change and human activities [4].

The Hulunbeier steppe's coverage once amounted to 70% in the early 1960s, but decreased to 35% in the 2000s [5]. As large areas of the steppe were transformed into cultivated land, the surface layer of the steppe deteriorated, resulting in a substantial loss of top soil, in turn leading to desertification [5]. The most fundamental causes of this desertification were dry weather, high temperatures resulting from global warming, and the relentless exploitation of water resources. For example, the mean air temperature increased by 1.1 °C, with a corresponding 54 mm reduction in annual rainfall, from 1950 to 1980, leading to a decrease in precipitation and an increase in evaporation [6]. This rendered the dry, exposed soil more susceptible to wind erosion. The grasslands have also been ruthlessly exploited, with overcultivation and overgrazing both occurring [7].

A project to combat and prevent desertification in the Hulunbeier steppe began in 2005 with sand dune fixation, and continued with tree plantation in 2009. The main species of tree that was planted was the Mongolian pine (*Pinus sylvestris* var. *mongolica*). Numerous studies were carried out to evaluate the effects of the project on the Hulunbeier area. A study using remote sensing images showed that the sand dune area decreased and vegetation increased after the project began [4]. In 2018, [8] reported that governmental policies and programs for steppe protection were having a positive effect. However, since 2016, the number of dead trees in Mongolian pine plantations has sharply increased.

The Mongolian pine is native to the Daxinganling Mountains and Hulunbeier sandy plain of China, as well as to areas of Russia and Mongolia (N 46°30'–N 53°59', E 118°00'–E 130°08'). It is a geographical variety of Scots pine (*Pinus sylvestris* L.), which is known to be one of the most drought-resistant tree species in central Europe [9]. The Mongolian pine features a straight trunk, is tolerant against infertile soil and sandy land, and can reduce wind damage and soil erosion. Accordingly, China has made efforts to restore forests using the Mongolian pine, which is the most suitable coniferous tree species for constructing protective plantations on sandy land [10]. The increase in the number of tree deaths on Mongolian pine plantations may be attributed to a lack of water on the sandy land in this arid climate [11]. Water is one of the most important limiting factors in the survival and growth of trees on sandy land [10], where its two main sources are precipitation and underground reservoirs [10,12].

In arid regions, soil moisture is affected primarily by groundwater, because of low precipitation and high evaporation [13–15]. Studies show that soil moisture decreases significantly with increased groundwater depth [12,16,17]. An increasingly dry climate leads to significantly reduced groundwater levels, and *Populus euphratica* and *Tamarix* spp. exposed to drought stress have been severely affected, or even killed in recent years [18,19]. As sand dunes increase in height, it becomes harder for trees to reach groundwater, which reduces their survival rate and growth [12]. This phenomenon was observed in the Taklamakan desert dunes, where the growth of trees has decreased as the dunes have become taller [20]. Plants are known to show improved water use efficiency under drought conditions [21–23]. One major change seen during drought stress is a reduction in plant height, which decreases the water transport distance from root to leaf [24–26]. In 2010, [27] suggested that the intrinsic water use efficiency (iWUE) and leaf mass per leaf unit area (LMA) of leaves differs among tree species, possibly according to growth patterns and susceptibility to drought stress in semiarid conditions. However, although physiological analysis of iWUE has recently been performed using tree rings and leaves [22,23], no studies have analyzed the effects of sand dune height on tree growth in arid and semiarid areas. In addition, species are being selected for transplantation in areas such as grasslands and sand dunes without full regard for the natural environment.

The objective of this study is to analyze and compare markers of tree growth, iWUE, and the survival rate of the Mongolian pine according to changes in sand dune height. We hypothesized that an increase in sand dune height, with a concomitant increase in the distance to groundwater, may lead to a decrease in survival rate. These findings could inform the selection of appropriate species for plantation in semiarid and arid environments. To test our hypothesis, we measured the growth

and survival rates, leaf area, leaf length, LMA, and iWUE of Mongolian pine trees at different sand dune heights.

2. Materials and Methods

2.1. Study Site and Experimental Design

The study area is located in the sand dunes of the Hulunbeier steppe. Two-year old Mongolian pine seedlings were used in this study. The area was protected from livestock and wild animals by a barbed wire fence. The altitude of the surrounding lakes was 576 m and the maximum height of the sand dunes was 593 m. The elevation of the lake within 500 m of the survey site was 576.6 m. The geographic coordinates and elevation of each measurement point were recorded using a global positioning system (GPS). The distance between tree specimens and the lake, as well as the height of the sand dunes, was analyzed using the GPS coordinates (ArcGIS 10.6, ESRI, Redlands, USA).

The annual rainfall in Hulunbeier is 288 mm, 92.0% of which falls between April and October. This region has a semidry climate, with a monthly mean temperature ranging from $-23.2\text{ }^{\circ}\text{C}$ in January to $21.7\text{ }^{\circ}\text{C}$ in July. The monthly mean relative humidity ranges from 76.8% in December to 41.7% in May, and the mean wind speed ranges from 12.8 m s^{-1} in April to 7.9 m s^{-1} in January. These values were extrapolated from meteorological data recorded between 1987 and 2016 at the Amgalang County Meteorological Station (N $48^{\circ}12'$, E $118^{\circ}15'$; elevation: 641 m) and the nearest experimental sites, maintained by the China Meteorological Administration. The annual evaporative water loss is 1400–1900 mm. The soil area in the Hulunbeier steppe is located between N $47^{\circ}20'$ and N $49^{\circ}59'$ and E $117^{\circ}10'$ and E $121^{\circ}12'$. It covers an area of $43,000\text{ km}^2$ and is 270 km in length from east to west and 170 km from north to south. The eastern zone is mostly comprised of chernozem soil, the middle zone has dark chernozem soil, the western zone has chestnut and light chestnut soils, and the gouge zone has Aeolian sandy soil. The region has a high sand content, especially of fine sand. Aeolian sandy soil is distributed throughout the sandy land and sandy plains in the outer regions of the steppe [5].

We selected a 2 ha area within the study area in 2013, wherein there were 5 measurement points corresponding to different sand dune heights. Each point consisted of three $40.0 \times 4.0\text{ m}^2$ areas, spaced 20 m apart along the sand dune. The sand dune height increased by a total of 6.2 m between points P1 and P5. The spacing between the Mongolian pine seedlings was 3.0–4.0 m, and the density of the trees was 833 trees/ha^{-1} . Each point contained 30 trees (Figure 1).

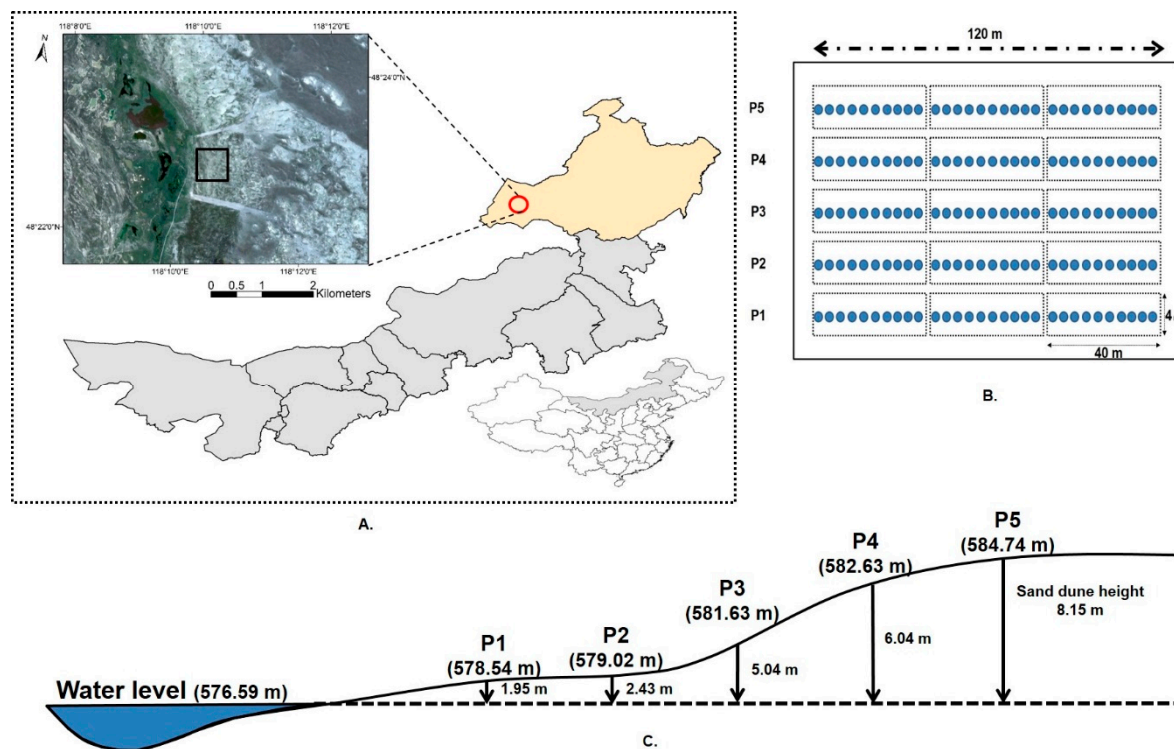


Figure 1. Study area and sampling sites in Hulunbeier, China. (A) Red circle: Location of the 2005 desertification combating project; black square: sampling sites for carbon isotope and intrinsic water use efficiency (iWUE) analysis. (B) Location of the tree growth belt and 15 plots. (C) Vertical distance to the groundwater level. Sand dune height was measured above the level of the surrounding lake.

2.2. Soil Moisture

To measure soil moisture, a moisture sensor (Waterscout SM100, Spectrum Technologies, Aurora, USA) was installed at each point, with moisture recorded at soil depths of 10, 30, 50, and 80 cm. The sensor at P1 was installed in August 2016, while the sensors at P2–P5 were installed in July 2018.

2.3. Survival Rate, Tree Growth, Pine Needle Features, and LMA

We assessed 30 trees at each measurement point. The tree height (m), diameter at root collar (DRC) (cm), diameter at breast height (DBH) (cm), longest shoot length (cm), and survival rate (%) were measured in July 2018 after 9 growing seasons.

At each survey site in July 2017, 30 pine needles were acquired for measurement of pine needle length, area, and width. The needles were collected at a height of 2 m, from a southerly location in which they were fully exposed to sunlight. The area (cm²), length (cm), and width (cm) of the pine needles were measured using a V700 Photo Scanner (EPSON, Japan) and the WinSeedle software program (Regent Instruments, Québec, Canada). The LMA was calculated by dividing the dry leaf mass by the leaf area [28]. The leaves were then dried in an oven (72 °C, 48 h) and weighed to 0.0001 g using an electronic microscale (Balance XS204, Mettler Toledo, Columbus, USA) to obtain the dry leaf mass.

2.4. Carbon Isotope Analysis and iWUE

To estimate the water use efficiency of the trees at each measurement point, 2 needles were collected from each of 3 trees. After drying for 72 hours at 65 °C, the foliar carbon isotope composition (¹³C) of the needles was analyzed using Equation (1). Measurements were taken using a stable isotope ratio mass spectrometer system with an elemental analyzer (Vision-EA, Isoprime, Cheadle, Hulme, UK). Global

daily atmospheric CO₂ data were obtained from the Earth System Research Laboratory (ESRL; National Oceanic & Atmospheric Administration; http://www.esrl.noaa.gov/gmd/ccgg/trends/gl_data.html).

$$\delta^{13}\text{C} (\text{‰}) = \left\{ \frac{\left[\left(\frac{\delta^{13}\text{C}}{\delta^{12}\text{C}} \right)_{\text{sample}} - \left(\frac{\delta^{13}\text{C}}{\delta^{12}\text{C}} \right)_{\text{standard}} \right]}{\left(\frac{\delta^{13}\text{C}}{\delta^{12}\text{C}} \right)_{\text{standard}}} \right\} \times 1000 \text{ ‰} \quad (1)$$

The C_i/C_a ratio was calculated using Equation (2), from [29] with some modifications [30].

$$\frac{C_i}{C_a} = \frac{\delta_{\text{atm}} - \delta^{13}\text{C} - a}{b - a} \quad (2)$$

In Equation (2), δ_{atm} indicates the ¹³CO₂ distribution in the atmosphere (−7.8‰), a represents the diffusivity of ¹³CO₂ in atmosphere (mol) ($a = 4.4\text{‰}$), and b represents discrimination by Rubisco against ¹³CO₂ ($b = 27\text{‰}$).

The iWUE was determined using Equation (3) [31,32].

$$\text{iWUE} (\mu\text{mol mol}^{-1}) = \frac{C_a - C_i}{1.6} = \frac{C_a(b - \delta^{13}\text{C})}{1.6(b - a)} \quad (3)$$

Here, C_a indicates the ambient CO₂ concentration ($C_a = 405.39$ ppm) and C_i indicates the intercellular CO₂ concentration (ppm). The ratio of diffusivities between water vapor and CO₂ in the atmosphere is represented by 1.6.

2.5. Statistical Analyses

SPSS software (version 22.0; IBM Corp, New York, USA) was used for all data analyses. The significance level was set at $p \leq 0.05$. One-way ANOVA was performed to compare the physiological variables of the trees among the sand dune height measurement points, and the Shapiro–Wilk normality test was used to determine the normality of the distribution of the data. In cases with a normal distribution, a post hoc test was performed (equal variance, Duncan’s multiple range test; unequal variance, Dunnett’s T3 test). In all other cases, nonparametric tests (Jonckheere–Terpstra test and Mann–Whitney test) were used, with $\alpha = 0.05$. Since soil moisture is in large part supplied through underground water in arid areas, we also measured the correlation between soil moisture and iWUE at each soil depth.

3. Results

3.1. Soil Moisture

The soil moisture was measured at depths of 10 cm ($5.96\% \pm 2.78\%$), 30 cm ($5.04\% \pm 4.30\%$), 50 cm ($14.21\% \pm 10.19\%$), and 80 cm ($21.99\% \pm 12.94\%$) from August 2016 to September 2018. The soil moisture increased with an increase in soil depth at P1 and P2, whereas the opposite was true at P3–P5. The largest difference in soil moisture among measurement points was observed at a depth of 80 cm (Figure 2).

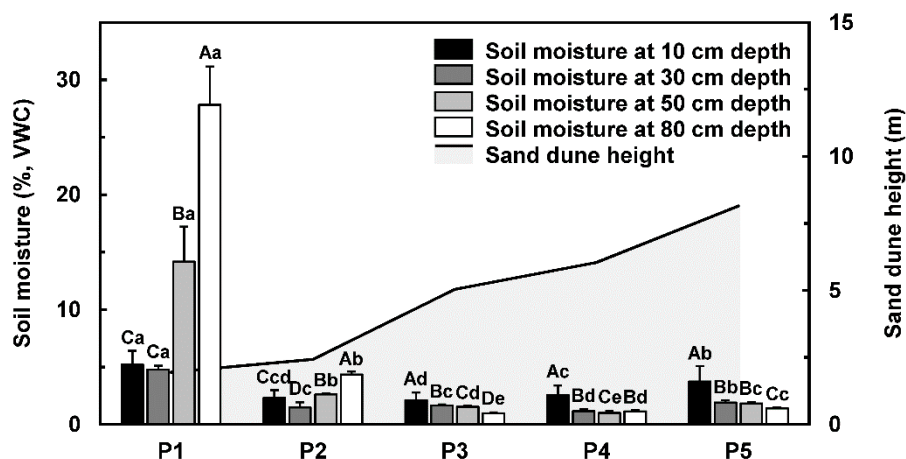


Figure 2. Moisture contents at different soil depths according to changes in sand dune height, from July to September 2018. Values with different capital letters indicate significant differences among four soil depths in each measurement point (Dunnett's T3 test, $p \leq 0.05$). Values with different small letters denote significant differences among five measurement points in each soil depth (Dunnett's T3 test, $p \leq 0.05$). Soil moisture data at 50 cm in P1 was not available from July to September 2018, so data from 2017 was used for the same period.

3.2. Survival Rate

The survival rate was highest (100%) at P2 and lowest (40%) at P4 and P5; a significant difference in survival rate was observed among the measurement points ($p < 0.01$) (Figure 3). Trees planted at a sand dune height of 5.04 m or more were the most severely damaged by a 2016 drought, while trees at a sand dune height of 2.43 m or less were the least affected. The survival rate at measurement points P3–P5 decreased by an average of 26.7% from 2016 to 2018.

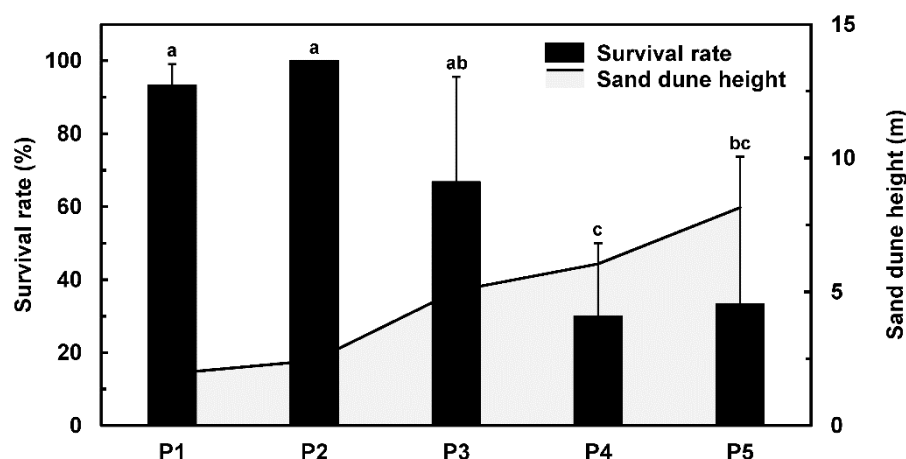


Figure 3. Survival rate of Mongolian pines planted for nine growing seasons according to changes in sand dune height. Values with different small letters denote significant differences among five measurement points (Jonckheere–Terpstra test, $p \leq 0.05$).

3.3. Tree Growth Characteristics

The most striking result was the significant difference in tree growth among measurement points ($p < 0.05$). Tree height was highest at P2 ($3.77 \text{ m} \pm 0.12 \text{ m}$) and lowest at P4 ($1.73 \text{ m} \pm 0.77 \text{ m}$). The average DRC was largest at P2 ($9.48 \text{ cm} \pm 0.18 \text{ cm}$) and smallest at P4 ($4.75 \text{ cm} \pm 0.93 \text{ cm}$). P2 had the largest DBH ($6.79 \text{ cm} \pm 0.41 \text{ cm}$), while that of P5 was the smallest ($1.98 \text{ cm} \pm 0.94 \text{ cm}$). The longest average shoot length was seen at P2 ($19.63 \text{ cm} \pm 3.69 \text{ cm}$), while the shortest was seen at P5 ($6.21 \text{ cm} \pm 2.32 \text{ cm}$). Growth characteristics showed an inverse relationship with sand dune height (Table 1).

Table 1. Growth responses of Mongolian pines planted for nine growing seasons according to changes in sand dune height. Tree height: Values with different small letters indicate significant differences (Jonckheere–Terpstra test, $p \leq 0.05$). Diameter at root collar (DRC), diameter at breast height (DBH): Values with different small letters denote significant differences (Dunnett’s T3 test, $p \leq 0.05$). Shoot length: Values with different small letters represent significant differences (Duncan’s multiple range test, $p \leq 0.05$).

Point	1	2	3	4	5
Tree height (m)	3.45 ± 0.27 a	3.77 ± 0.12 a	2.17 ± 1.26 b	1.73 ± 0.38 b	1.82 ± 0.47 b
DRC (cm)	8.81 ± 0.66 a	9.48 ± 0.18 a	6.52 ± 2.78 b	4.75 ± 0.93 c	5.24 ± 1.54 bc
DBH (cm)	6.14 ± 0.35 ab	6.79 ± 0.41 a	3.64 ± 2.72 b	2.09 ± 0.75 c	1.98 ± 0.94 c
Shoot length (cm)	18.91 ± 3.48 a	19.63 ± 3.69 a	14.12 ± 2.93 a	7.87 ± 4.13 b	6.21 ± 2.32 b

3.4. Pine Needle Characteristics, Carbon Isotope Composition, and iWUE

The average pine needle area and length decreased with increasing sand dune height. Leaf area, length, and width were significantly different ($p < 0.001$) between current- (2017) and one-year-old (2016) pine needles. The leaf area, length, and width of leaves were different from current- and one-year-old pine needles with each point except p1 point leaf length ($p < 0.05$). The largest leaf area of current-year pine needles was seen at P1 ($1.09 \text{ cm}^2 \pm 0.20 \text{ cm}^2$) and the smallest at P5 ($0.53 \text{ cm}^2 \pm 0.10 \text{ cm}^2$), while for one-year-old pine needles, the largest leaf area was at P2 ($1.34 \text{ cm}^2 \pm 0.19 \text{ cm}^2$) and the smallest was at P4 ($0.77 \text{ cm}^2 \pm 0.11 \text{ cm}^2$). The leaf length of current-year pine needles was longest at P2 ($6.03 \text{ cm} \pm 0.74 \text{ cm}$) and shortest at P3 ($3.84 \text{ cm} \pm 0.40 \text{ cm}$). For one-year-old pine needles, the longest leaf length was seen at P2 ($6.70 \text{ cm} \pm 0.80 \text{ cm}$) and the shortest at P4 ($4.53 \text{ cm} \pm 0.64 \text{ cm}$). The leaf width of current-year pine needles was largest at P1 ($0.23 \text{ cm} \pm 0.02 \text{ cm}$) and smallest at P5 ($0.17 \text{ cm} \pm 0.02 \text{ cm}$), while in one-year-old pine needles it was largest at P2 ($0.28 \text{ cm} \pm 0.05 \text{ cm}$) and smallest at P5 ($0.23 \text{ cm} \pm 0.03 \text{ cm}$) (Figure 4). The LMA of the current- and one-year-old pine needles showed no significant difference according to sand dune height ($p > 0.05$).

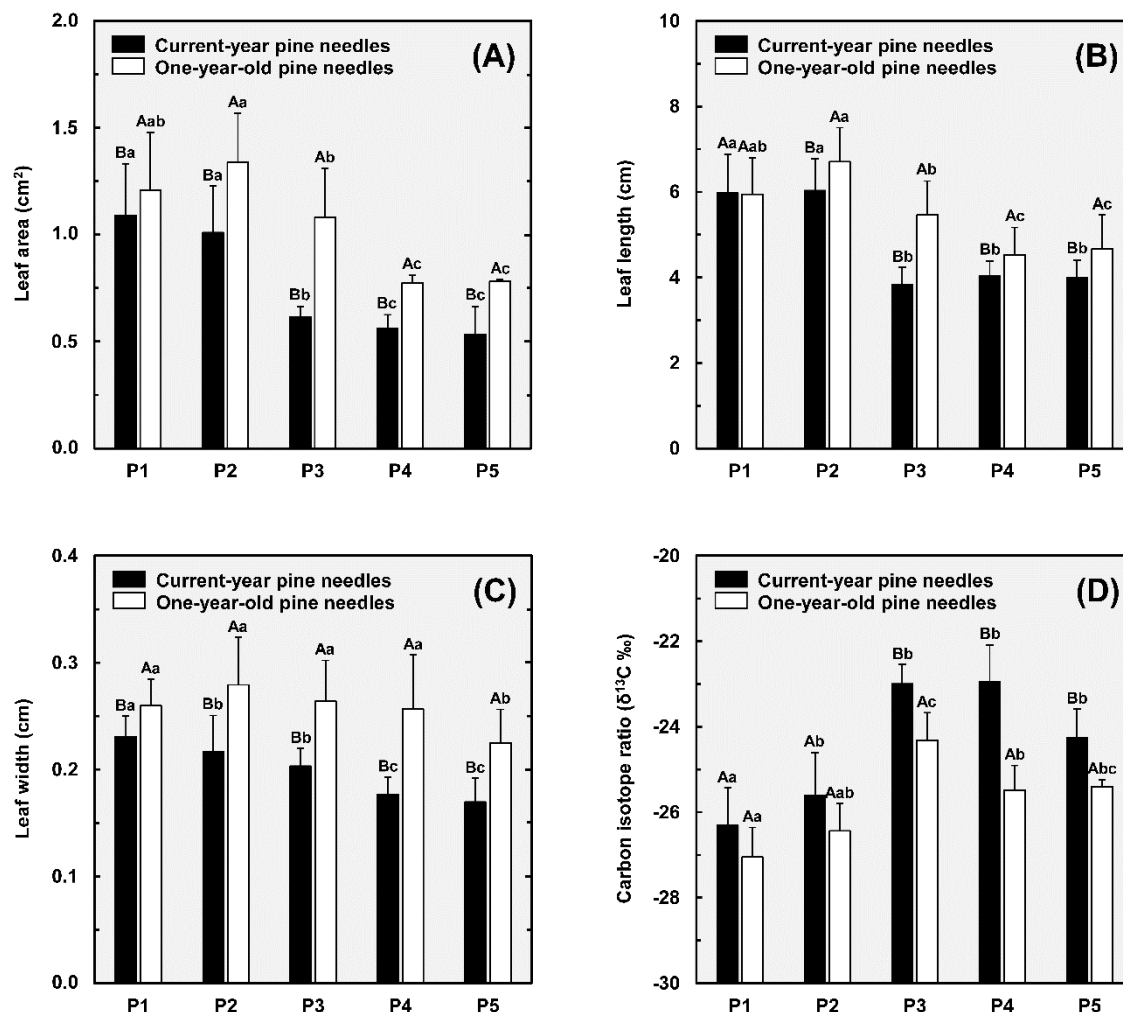


Figure 4. Comparison of Mongolian pine needle characteristics, i.e., leaf area (A), length (B), width (C), and carbon isotope ratios (D), according to changes in sand dune height. Values with different capital letters indicate significant differences between two needles age classes in each measurement point (Mann–Whitney test, $p \leq 0.05$). Values with different small letters denote significant differences among five measurement points in each needle age class (Jonckheere–Terpstra test, $p \leq 0.05$).

The $\delta^{13}\text{C}$ analysis of current-year pine needle samples showed a significant difference at P3. The current-year pine needles at P1 ($-26.31\text{‰} \pm 0.88\text{‰}$) and P2 ($-25.60\text{‰} \pm 0.99\text{‰}$) showed similar $\delta^{13}\text{C}$ values to each other, while those at P3 ($-23.00\text{‰} \pm 0.46\text{‰}$), P4 ($-22.94\text{‰} \pm 0.85\text{‰}$), and P5 ($-24.25\text{‰} \pm 0.66\text{‰}$) were higher. One-year-old pine needles showed a significant difference among measurement points: P1 ($-27.05\text{‰} \pm 0.69\text{‰}$), P2 ($-26.44\text{‰} \pm 0.64\text{‰}$), P3 ($-24.32\text{‰} \pm 0.64\text{‰}$), P4 ($-25.48\text{‰} \pm 0.57\text{‰}$), and P5 ($-25.41\text{‰} \pm 0.16\text{‰}$) ($p < 0.05$) (Figure 4). One-year-old pine needles showed similar $\delta^{13}\text{C}$ values between P1 and P2, as did P3–P5, and the values were significantly different between P1 and P2 versus P3–P5 ($p < 0.05$). The $\delta^{13}\text{C}$ values were also significantly different between the current- and one-year-old pine needles at P3 to P5 ($p < 0.05$).

The iWUE was significantly different among the measurement points and increased as sand dune height increased ($p < 0.05$) (Figure 5). The iWUE for current-year pine needles at P1 ($95.18 \pm 9.87 \mu\text{mol CO}_2 \text{ mol}^{-1} \text{ H}_2\text{O}$) and P2 ($103.10 \pm 11.12 \mu\text{mol CO}_2 \text{ mol}^{-1} \text{ H}_2\text{O}$) was lower than at P3 ($132.29 \pm 5.12 \mu\text{mol CO}_2 \text{ mol}^{-1} \text{ H}_2\text{O}$), P4 ($132.96 \pm 9.54 \mu\text{mol CO}_2 \text{ mol}^{-1} \text{ H}_2\text{O}$), and P5 ($125.34 \pm 7.45 \mu\text{mol CO}_2 \text{ mol}^{-1} \text{ H}_2\text{O}$). The iWUE of one-year-old pine needles showed a similar trend, i.e., the values for P1 ($86.89 \pm 7.78 \mu\text{mol CO}_2 \text{ mol}^{-1} \text{ H}_2\text{O}$) and P2 ($93.76 \pm 7.16 \mu\text{mol CO}_2 \text{ mol}^{-1} \text{ H}_2\text{O}$) were lower than those for P3 ($117.53 \pm 7.18 \mu\text{mol CO}_2 \text{ mol}^{-1} \text{ H}_2\text{O}$), P4 ($104.49 \pm 6.43 \mu\text{mol CO}_2 \text{ mol}^{-1} \text{ H}_2\text{O}$),

and P5 ($105.33 \pm 1.82 \mu\text{mol CO}_2 \text{ mol}^{-1} \text{ H}_2\text{O}$). The iWUE was also significantly different between the current- and one-year-old pine needles at P3 to P5 ($p < 0.05$).

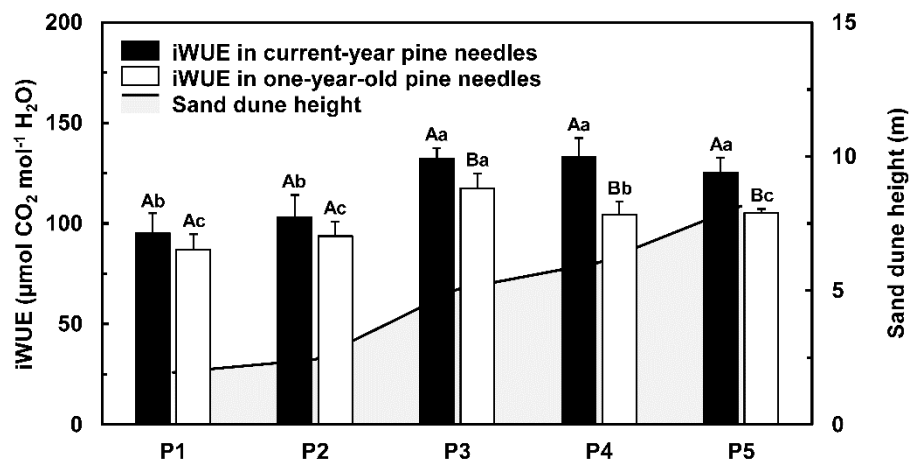


Figure 5. Comparison of iWUE values in Mongolian pine needles according to changes in sand dune height. Values with different capital letters indicate significant differences between two needle age classes in each measurement point according (Mann-Whitney test, $p \leq 0.05$). Values with different small letters denote significant differences among five measurement points in each needle age class (Jonckheere–Terpstra test, $p \leq 0.05$).

4. Discussion

4.1. Increased iWUE and Reduced Leaf Area Correlates with Sand Dune Height

Plants are generally known to increase their iWUE to adapt to dry conditions [33–35]. It has been reported previously that Scots pine needle's stomatal density and iWUE are correlated with changes in temperature and CO₂ levels in arid climates [36]. A correlation between a dry climate and higher iWUE has also been reported in *Ulmus pumila* [22]. In our study, iWUE tended to increase as sand dune height increased, especially at P3 and above. P3 is where the groundwater level drops more than 1 m below the average Mongolian pine root depth. We determined that P3 corresponded to the dune height at which the groundwater supply became difficult or impossible to reach such that, in response, the trees increased their iWUE as a survival mechanism. In dry areas, trees depend on groundwater more so than on rainfall, such that subsoil moisture is of critical importance [37]. At a soil depth of 80 cm, there was a significant increase in iWUE relative to the other depths ($p < 0.05$) (Figure 6). Therefore, when selecting a location in which to plant trees in arid areas, the distance between the tree and the point at which it can access subsoil moisture needs to be considered more so than topsoil moisture.

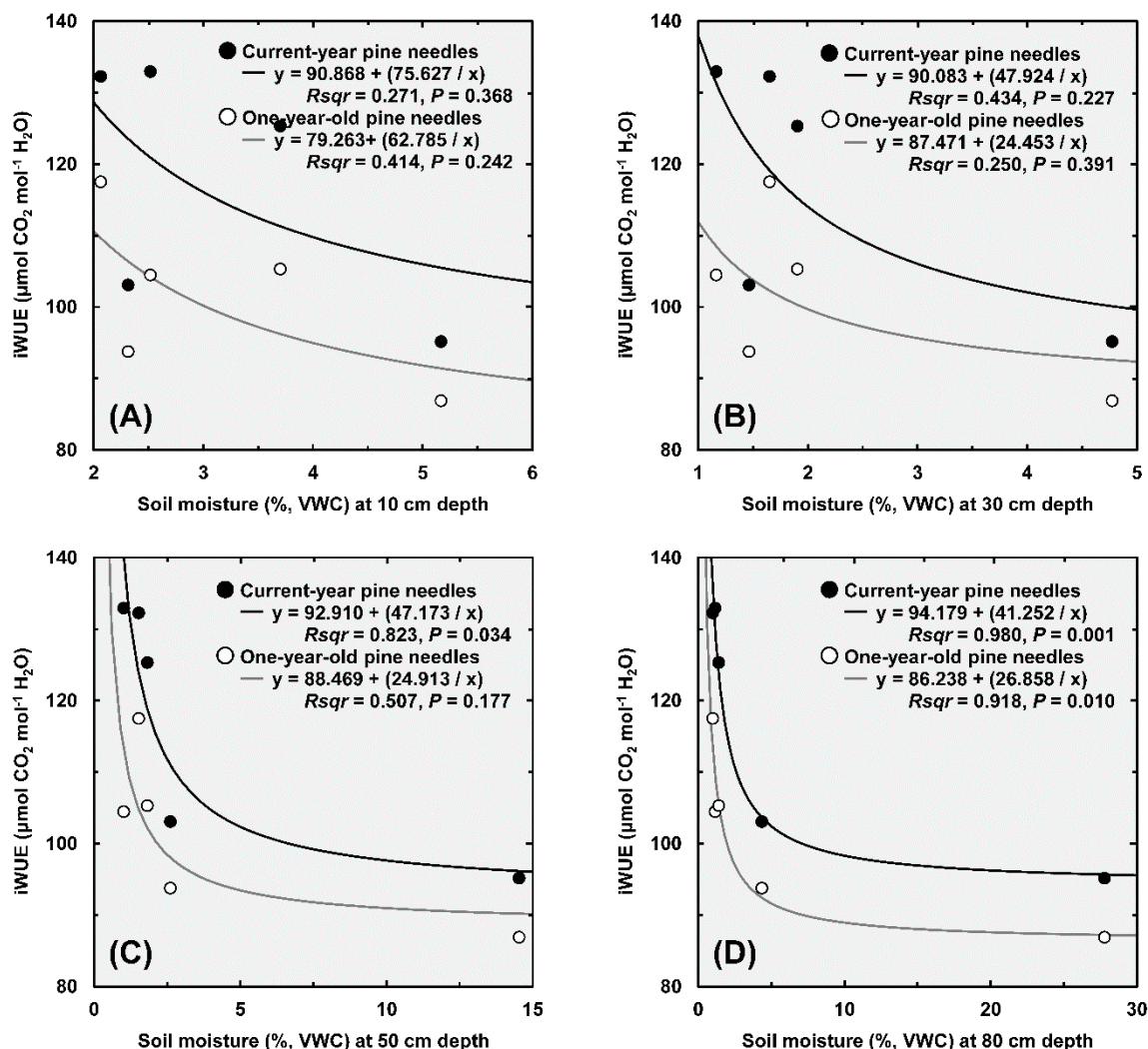


Figure 6. Relationship between iWUE values in Mongolian pine needles and moisture contents at different soil depths, i.e., 10 (A), 30 (B), 50 (C), and 80 cm (D), according to changes in sand dune height.

In this study, the area occupied by current- and one-year-old pine needles decreased from P1 and P2 to P3–P5 ($p < 0.05$). In addition, both the current- and one-year-old pine needle areas tended to decrease as sand dune height increased. Furthermore, the difference between current- and one-year-old pine needles was observed ($p < 0.05$), but both pine needles were affected by the height difference of the sand dune. In a similar study, the leaf area of *Populus euphratica* significantly decreased as sand dune height increased [20]. Dry-tolerant species also exhibit a lower C_i/C_a value than mesic species, due to lower discrimination against ¹³C [38]. Under drought stress, a plant can reduce its rate of transpiration by decreasing the leaf area [39]. Together, these strategies help the tree to reduce stomatal density and increase iWUE, improving the likelihood of survival in environments where the water supply is insufficient.

4.2. Reduced Survival and Growth of Mongolian Pine Correlates with Sand Dune Height

Temporary increases in iWUE help protect trees from drought, but prolonged increases inhibit growth, eventually leading to death [23]. Previous studies have found that intense drought stress significantly increases the risk of death among drought-stressed plants [40,41]. Soil dryness reduced leaf size in the Scots pine [42], which in turn not only reduced water loss but also the amount of photosynthate that was available for growth [43]. The Scots pine, *Populus simonii*, and other genera have been shown to grow significantly better and have a higher iWUE, in the early stages of drought,

before dying a few years later [44–46]. In this study, we thought the Mongolian pine's death was not related to the dramatic increase of water use efficiency. According to our observation, the Mongolian pine in our research site has already exceeded the extreme drought, considered a more critical factor of the death than the sudden increase of its water use efficiency in response to drought, like in previous studies [23,44–46].

Red leaves and dead trees were not seen during the 2016 survey, however, the following year there was an increase in tree mortality. A severe drought in August 2016 seems to have triggered these effects. Trees at measurement points P3–P5 were mainly affected, while those at P1 and P2 were not damaged. In this study, survival and growth decreased rapidly at P3 and above, where the soil water content was less than 5%. In sandy land, Mongolian pine roots reached an average vertical depth of 1.56 m, with 0.90 m of horizontal growth reported to occur after 13 years [10]. Based on three months of soil data, soil moisture was highest at P1, followed by P2, P3, P4, and P5, because as the height of the sand dunes increased from P1–P5, the distance from the trees to groundwater also increased. Thus, trees planted at P1 and P2 had a sufficient water supply even during extreme drought, whereas trees at P3–P5 showed decreased survival and growth because of insufficient water. Our results are consistent with a similar study that showed a strong relationship between monthly water level and biomass in *Pinus radiata* seedlings [47].

Studies on conifer restoration have shown that competition for water plays a crucial role in seedling survival and growth [48–54]. Preservation of soil moisture until early August is especially critical for seedling growth [55]. In our study, increased sand dune height led to an insufficient water supply at P3–P5, where the groundwater was more than 80 cm below the seedlings, resulting in a reduction in tree survival and growth rates.

5. Conclusions

Nine years after planting Mongolian pines at various sand dune heights, we saw significant variation in growth characteristics, such as tree height, DRC, DBH, leaf area, leaf length, and iWUE. As sand dune height increased, Mongolian pine trees increased their iWUE by decreasing their leaf area. However, there was no significant difference in LMA according to sand dune height. The Mongolian pine was able to adapt to survive at dryer sites, but prolonged exposure to inadequate moisture decreased the growth and survival rates of the trees. When planning an afforestation project in dry, sandy environments like the Hulunbeier steppe, herbaceous and shrubby plants that have a lower water requirement than trees should be considered. In the case of the Mongolian pine, care should be taken to avoid plantation in areas where soil moisture is less than 5% in subsoil.

Author Contributions: C.-B.K. and K.-H.P. proposed the study. C.-B.K. designed the study and carried out field work, data analysis, and manuscript preparation. Y.S.K., J.K., K.-H.P. and G.-L.G. contributed to the field surveys. J.K., S.K., and S.C. analyzed the leaf data. H.T.C. installed equipment such as soil moisture. Y.-F.B. analyzed the climate data. Y.S.K., Y.S., and J.K. reviewed the work.

Funding: This research was funded by National Institute of Forest Science (grant numbers FE0100-2018-02 and FE0604-2016-02).

Acknowledgments: We appreciate Seongwan Park for helping with our field surveys. We wish to thank Jiae An, Hanna Chang, and Seung Hyun Han for helping us with the laboratory experiments.

Conflicts of Interest: The authors declare no conflict of interest.

References

1. United Nations Convention to Combat Desertification (UNCCD). *Report of the Conference of the Parties on Its Thirteenth Session, Held in Ordos, China from 6 to 16 September 2017 Part One: Proceedings*; United Nations Convention to Combat Desertification: Ordos, China, 2017; pp. 1–36.
2. Adeel, Z.; Safriel, U.; Niemeijer, D.; White, R. *Millennium Ecosystem Assessment: Ecosystems and Human Well-Being: Desertification Synthesis*; World Resource Institute: Washington, DC, USA, 2005; pp. 1–36.

3. Wang, T.; Wu, W.; Xue, X.; Han, Z.; Zhang, W.; Sun, Q. Spatial-temporal changes of sandy desertified land during last 5 decades in Northern China. *Acta. Geogr. Sin.* **2004**, *59*, 203–212. (In Chinese)
4. Xu, D.; Song, A.; Li, D.; Ding, X.; Wang, Z. Assessing the relative role of climate change and human activities in desertification of North China from 1981 to 2010. *Front. Earth Sci.* **2019**, *13*, 43–54. [[CrossRef](#)]
5. Park, K.H.; Qu, Z.Q.; Wan, Q.Q.; Ding, G.D.; Wu, B. Effects of enclosures on vegetation recovery and succession in Hulunbeier steppe, China. *For. Sci Technol.* **2013**, *9*, 25–32. [[CrossRef](#)]
6. Lv, S.; Lu, X.; Jin, W. Studies on wind erosion desertification and methods of reversion in Hulunbeier Steppe. *J. Arid Land Resour. Environ.* **2005**, *19*, 59–63. (In Chinese)
7. Bo, T.L.; Fu, L.T.; Zheng, X.J. Modeling the impact of overgrazing on evolution process of grassland desertification. *Aeolian Res.* **2013**, *9*, 183–189. [[CrossRef](#)]
8. Zhao, H.; Zhao, Y.; Gao, G.; Ho, P. China's desertification deconstructed: Towards scientists' model based on long-term perceptions of grassland restoration (1995–2011). *Ecol. Restor.* **2018**, *26*, 26–36. [[CrossRef](#)]
9. Ellenberg, H. *Vegetation Ecology of Central Europe*; Cambridge University Press: Cambridge, UK, 1988; pp. 193–236.
10. Zhu, J.J.; Zeng, D.H.; Kang, H.Z.; Wu, X.G.; Fan, Z.P.; Jiang, F.Q.; Li, F.Q.; Wang, H.X.; Xu, H.; Tan, H.; et al. *Decline of Pinus Sylvestris Var. Mongolica Plantations on Sandy Land*; China Forestry Publisher: Beijing, China, 2005; pp. 1–264.
11. Zhu, J.; Kang, H.; Tan, H.; Xu, M.; Wang, J. Regeneration characteristics of natural *Pinus sylvestris* var. *mongolica* forests on sandy land in Honghuaerji. *J. For. Res.* **2005**, *16*, 253–259.
12. Zhang, X.L.; Guan, T.Y.; Zhou, J.H.; Cai, W.T.; Gao, N.N.; Du, H.; Jiang, L.H.; Lai, L.M.; Zheng, Y.R. Groundwater depth and soil properties are associated with variation in vegetation of a desert riparian ecosystem in an arid area of China. *Forests* **2018**, *9*, 34. [[CrossRef](#)]
13. Deng, L.; Wang, K.B.; Li, J.; Shangguan, Z. Effect of soil moisture and atmospheric humidity on both plant productivity and diversity of native grasslands across the loess plateau, China. *Ecol. Eng.* **2016**, *94*, 525–531. [[CrossRef](#)]
14. Yu, T.; Feng, Q.; Si, J.; Xi, H.; Li, Z.; Chen, A. Hydraulic redistribution of soil water by roots of two desert riparian phreatophytes in northwest China's extremely arid region. *Plant Soil.* **2013**, *372*, 297–308. [[CrossRef](#)]
15. Lu, Z.; Wei, Y.; Xiao, H.; Zou, S.; Ren, J.; Lyle, C. Trade-offs between midstream agricultural production and downstream ecological sustainability in the Heihe River basin in the past half century. *Agric. Water Manag.* **2015**, *152*, 233–242. [[CrossRef](#)]
16. Chen, Y.N.; Pang, Z.; Chen, Y.P.; Li, W.H.; Xu, C.C.; Hao, X.M.; Huang, X.; Huang, T.M.; Ye, Z.X. Response of riparian vegetation to water-table changes in the lower reaches of Tarim River, Xinjiang Uygur, China. *Hydrogeol. J.* **2008**, *16*, 1371–1379. [[CrossRef](#)]
17. Hao, X.M.; Li, W.H.; Huang, X.; Zhu, C.G.; Ma, J.X. Assessment of the groundwater threshold of desert riparian forest vegetation along the middle and lower reaches of the Tarim River, China. *Hydrol. Process.* **2010**, *24*, 178–186. [[CrossRef](#)]
18. Peng, X.M.; Xiao, S.C.; Xiao, H.L. Preliminary dendrochronological studies on *Populus euphratica* in the lower reaches of Heihe River basin in northwest China. *Dendrochronologia* **2013**, *31*, 242–249. [[CrossRef](#)]
19. Zhu, Y.H.; Chen, Y.N.; Ren, L.L.; Lu, H.S.; Zhao, W.Z.; Yuan, F.; Xu, M. Ecosystem restoration and conservation in the arid inland river basins of Northwest China: Problems and strategies. *Ecol. Eng.* **2016**, *94*, 629–637. [[CrossRef](#)]
20. Gries, D.; Zeng, F.; Foetzki, A.; Arndt, S.K.; Bruelheide, H.; Thomas, F.M.; Zhang, X.; Runge, M. Growth and water relations of *Tamarix ramosissima* and *Populus euphratica* on Taklamakan desert dunes in relation to depth to a permanent water table. *Plant Cell Environ.* **2003**, *26*, 725–736. [[CrossRef](#)]
21. Timofeeva, G.; Treydte, K.; Bugmann, H.; Rigling, A.; Schaub, M.; Siegwolf, R.; Saurer, M. Long-term effects of drought on tree-ring growth and carbon isotope variability in Scots pine in dry environment. *Tree Physiol.* **2017**, *37*, 1028–1041. [[CrossRef](#)] [[PubMed](#)]
22. Park, G.E.; Lee, D.K.; Kim, K.W.; Batkhuu, N.O.; Tsogtbaatar, J.S.; Zhu, J.J.; Jin, Y.H.; Park, P.S.; Hyun, J.O.; Kim, H.S. Morphological characteristics and water-use efficiency of Siberian elm tree (*Ulmus pumila* L.) within arid regions of Northeast Asia. *Forests* **2016**, *7*, 280. [[CrossRef](#)]
23. Sun, S.J.; Qiu, L.F.; He, C.X.; Li, C.Y.; Zhang, J.S.; Meng, P. Drought-affected *Populus simonii* Carr. Show lower growth and long-term increases in intrinsic water-use-efficiency prior to tree mortality. *Forests* **2018**, *9*, 564. [[CrossRef](#)]

24. Ryan, M.G.; Yoder, B.J. Hydraulic limits to tree height and tree growth. *Bioscience* **1997**, *47*, 235–242. [[CrossRef](#)]
25. Mencuccini, M. The ecological significance of long-distance water transport: Short-term regulation, long-term acclimation and the hydraulic costs of stature across plant life forms. *Plant Cell Environ.* **2003**, *26*, 163–182. [[CrossRef](#)]
26. Addington, R.N.; Donovan, L.A.; Mitchell, R.J.; Vose, J.M.; Pecot, S.D.; Jack, S.B.; Hacke, U.G.; Sperry, J.S.; Oren, R. Adjustments in hydraulic architecture of *Pinus palustris* maintain similar stomatal conductance in xeric and mesic habitats. *Plant Cell Environ.* **2006**, *29*, 535–545. [[CrossRef](#)] [[PubMed](#)]
27. Tanaka-Oda, A.; Kenzo, T.; Koretsune, S.; Sasaki, H.; Fukuda, K. Ontogenetic changes in water-use efficiency ($\delta^{13}\text{C}$) and leaf traits differ among tree species growing in a semiarid region of the Loess Plateau, China. *For. Ecol. Manag.* **2010**, *259*, 953–957. [[CrossRef](#)]
28. Poorter, H.; Niinemets, U.; Pooter, L.; Wright, I.J.; Villar, R. Causes and consequences of variation in leaf mass per area (LMA): A meta-analysis. *New Phytol.* **2009**, *182*, 565–588. [[CrossRef](#)]
29. Farquhar, G.D.; O’Leary, M.H.; Berry, J.A. On the relationship between carbon isotope discrimination and the intercellular carbon dioxide concentration in leaves. *Funct. Plant Biol.* **1982**, *9*, 121–137. [[CrossRef](#)]
30. Korol, R.L.; Kirschbaum, M.U.F.; Farquhar, G.D.; Jeffreys, M. Effects of water status and soil fertility on the C-isotope signature in *Pinus radiata*. *Tree Physiol.* **1999**, *19*, 551–562. [[CrossRef](#)]
31. Saurer, M.; Siegwolf, R.W.; Schweinfurber, F.H. Carbon isotope discrimination indicates improving water-use efficiency of trees in northern Eurasia over the last 100 years. *Glob. Chang. Biol.* **2004**, *10*, 2109–2120. [[CrossRef](#)]
32. Farquhar, G.D.; Richards, R. Isotopic composition of plant carbon correlates with water-use-efficiency of wheat genotypes. *Funct. Plant Biol.* **1984**, *11*, 539–552. [[CrossRef](#)]
33. McDowell, N.; Allen, C.D.; Marshall, L. Growth, carbon-isotope discrimination, and drought-associated mortality across a *Pinus ponderosa* elevational transect. *Glob. Chang. Biol.* **2010**, *16*, 399–415. [[CrossRef](#)]
34. Nock, C.A.; Baker, P.J.; Wanek, W.; Leis, A.; Grabner, M.; Bunyavejchewin, S.; Hietz, P. Long-term increases in intrinsic water-use efficiency do not lead to increased stem growth in a tropical monsoon forest in western Thailand. *Glob. Chang. Biol.* **2011**, *17*, 1049–1063. [[CrossRef](#)]
35. Levesque, M.; Siegwolf, R.; Saurer, M.; Eilmann, B.; Rigling, A. Increased water-use efficiency does not lead to enhanced tree growth under xeric conditions. *New Phytol.* **2014**, *203*, 94–109. [[CrossRef](#)] [[PubMed](#)]
36. Beerling, D.J. Carbon isotope discrimination and stomatal responses of mature *Pinus sylvestris* L. trees exposed in situ for three years to elevated CO_2 and temperature. *Acta Oecol.* **1997**, *18*, 697–712. [[CrossRef](#)]
37. Fu, A.H.; Chen, Y.N.; Li, W.H. Water use strategies of the desert riparian forest plant community in the lower reaches of Heihe River Basin, China. *Sci. China Earth Sci.* **2014**, *57*, 1293–1305. [[CrossRef](#)]
38. Brodribb, T. Dynamics of changing intercellular CO_2 concentration during drought and determination of minimum functional Ci . *Plant Physiol.* **2006**, *111*, 179–185. [[CrossRef](#)] [[PubMed](#)]
39. Delucia, E.H.; Maherali, H.; Carey, E.V. Climate-driven changes in biomass allocation in pines. *Glob. Chang. Biol.* **2000**, *6*, 587–593. [[CrossRef](#)]
40. Greenwood, S.; Ruiz-Benito, P.; Martínez-Vilalta, J.; Lloret, F.; Kitzberger, T.; Allen, C.D.; Fensham, R.; Laughlin, D.C.; Kattge, J.; Bönsch, G.; et al. Tree mortality across biomes is promoted by drought intensity, lower wood density and higher specific leaf area. *Ecol. Lett.* **2017**, *20*, 539–553. [[CrossRef](#)] [[PubMed](#)]
41. Navarro-Cerrillo, R.; Rodríguez-Vallejo, C.; Silveiro, E.; Hortal, A.; Palacios-Rodríguez, G.; Duque-Lazo, J.; Camarero, J. Cumulative drought stress leads to a loss of growth resilience and explains higher mortality in planted than in naturally regenerated *Pinus pinaster* stands. *Forests* **2018**, *9*, 358. [[CrossRef](#)]
42. Giuggiola, A.; Zweifel, R.; Feichtinger, L.M.; Vollenwider, P.; Bugmann, H.; Haeni, M.; Rigling, A. Competition for water in a xeric forest ecosystem—Effects of understory removal on soil micro-climate, growth and physiology of dominant Scots pine trees. *For. Ecol. Manag.* **2018**, *409*, 241–249. [[CrossRef](#)]
43. Oberhuber, W.; Stumbeck, M.; Kofler, W. Climate-tree-growth relationships of Scots pine stands (*Pinus sylvestris* L.) exposed to soil dryness. *Trees* **1998**, *13*, 19–27. [[CrossRef](#)]
44. Levanic, T.; Cater, M.; McDowell, N.G. Associations between growth, wood anatomy, carbon isotope discrimination and mortality in *Quercus robur* forest. *Tree Physiol.* **2011**, *31*, 298–308. [[CrossRef](#)]
45. Moran-Lopez, T.; Poyatos, R.; Llorens, P.; Sabate, S. Effects of past growth trends and current water use strategies on Scots pine and pubescent oak drought sensitivity. *Eur. J. For. Res.* **2014**, *133*, 369–382. [[CrossRef](#)]

46. Hentschel, R.; Rosner, S.; Kayler, Z.E.; Andreassen, K.; Børja, I.; Solberg, S.; Tveito, O.E.; Priesack, E.; Gessler, A. Norway spruce physiological and anatomical predisposition to dieback. *For. Ecol. Manag.* **2014**, *322*, 27–36. [[CrossRef](#)]
47. Watt, M.S.; Whitehead, D.; Mason, E.G.; Richardson, B.; Kimberley, M.O. The influence of weed competition for light and water on growth and dry matter partitioning of young *Pinus radiata* at a dryland site. *For. Ecol. Manag.* **2003**, *183*, 363–376. [[CrossRef](#)]
48. Newton, M.; Preest, D.S. Growth and water relations of Douglas fir (*Pseudotsuga menziesii*) seedlings under different weed control regimes. *Weed Sci.* **1988**, *36*, 653–662. [[CrossRef](#)]
49. Powers, R.; Reynolds, P.E. Ten-year responses of ponderosa pine plantations to repeated vegetation and nutrient control along an environmental gradient. *Can. J. For. Res.* **1999**, *29*, 1027–1038. [[CrossRef](#)]
50. Mason, E.G.; Rose, R.; Rosner, L.S. Time vs. light: A potentially useable light sum hybrid model to represent the juvenile growth of Douglas-fir subject to varying levels of competition. *Can. J. For. Res.* **2007**, *37*, 795–805. [[CrossRef](#)]
51. Dinger, E.J.; Rose, R. The integration of soil moisture, xylem water potential, and fall-spring herbicide treatments to achieve the maximum growth response in newly planted Douglas-fir seedlings. *Can. J. For. Res.* **2009**, *39*, 1401–1414. [[CrossRef](#)]
52. Dinger, E.J.; Rose, R. Initial autumn-spring vegetation management regimes improve moisture conditions and maximize third-year Douglas-fir seedling growth in a Pacific Northwest plantation. *N. Z. J. For. Sci.* **2010**, *40*, 93–108.
53. Maguire, D.A.; Mainwaring, D.B.; Rose, R.; Garber, S.M.; Dinger, E.J. Response of coastal Douglas-fir and competing vegetation to repeated and delayed weed control treatments during early plantation development. *Can. J. For. Res.* **2009**, *39*, 1208–1219. [[CrossRef](#)]
54. Pinto, J.R.; Marshall, J.D.; Dumroese, R.K.; Davis, A.S.; Cobos, D.R. Photosynthetic response, carbon isotopic composition, survival, and growth of three stock types under water stress enhanced by vegetative competition. *Can. J. For. Res.* **2012**, *42*, 333–344. [[CrossRef](#)]
55. Carlos, A.G.B.; Eric, J.D. Use of water stress integral to evaluate relationships between soil moisture, plant water stress and stand productivity in young Douglas-fir trees. *New For.* **2018**, *49*, 775–789.



© 2019 by the authors. Licensee MDPI, Basel, Switzerland. This article is an open access article distributed under the terms and conditions of the Creative Commons Attribution (CC BY) license (<http://creativecommons.org/licenses/by/4.0/>).